Parametric Study of Size and Surface Effects on Concentrations of Thermally Excited Charge Carriers

Isaac Greber[1]
John C. Angus[2]
[1]Department of Mechanical and Aerospace Engineering
[2] Department of Chemical and Biomolecular Engineering
Case Western Reserve University
Cleveland, Ohio
[1]phone: (1) 216-368-6451
[2]phone (1) 216-368-4133
e-mail: isaac.greber@case.edu
e-mail: john.angus@case.edu

***Abstract*— Electrons excited into conductive states by thermal processes or by ultraviolet light can undergo independent de-activation processes in the bulk or on surfaces. Therefore, differences in size and surface morphology can lead to different overall bulk and surface de-activation rates. For thermally excited charge carriers this difference leads to higher excited electron concentrations (and hence higher Fermi energies) in objects with smoother surfaces than in otherwise identical objects with rougher surfaces. Similarly, higher excited electron concentrations are expected in larger than in smaller particles. These predictions are in general agreement with prior and current experimental observations of tribo-electric charge transfer. For silica-based solids, modeling of the excitation, diffusional transport, and de-excitation shows that surface features in the tens of micron size range lead to significant differences in excited electron concentration. This symmetry breaking effect can take place in parallel with other processes and may also play a role in the charging of solids of different compositions.**

I. INTRODUCTION

Despite its importance in many fields, electrostatic charging of particles of different size and surface roughness, but with identical composition, remains poorly understood [1-8]. In a previous paper [1] we considered size effects in spherical particles under optical excitation. The spatial concentration distribution of excited electrons arises from their diffusion from the excitation site and subsequent de-excitation within the bulk or at the surface. We showed how the relative rates of bulk and surface de-excitation are size dependent and influence the concentration of excited electrons and hence the Fermi level and magnitude and direction of charge transfer between particles. Here we expand on those quasi one-dimensional studies and determine the spatial distribution of thermally excited electrons in generalized cylindrical and hemispherical geometries.

II. DISCUSSION

A. Excitation Processes

There are numerous possible types of excitation in crystalline solids containing defects, each with different consequences for charge carrier conductivity. Excitation of electrons from the valence to the conduction band leaves equal numbers of excited electrons in the conduction band and holes in the valence band. Excitation of electrons from fixed donor sites to the conduction band leaves fixed, positively charged donor sites. Electrons can also be excited from the valence band to fixed acceptor sites leaving valence band holes and negatively charged acceptor sites. Furthermore, for sufficiently large concentrations of defects, impurity bands can form that can support conductivity.

The ultraviolet end of the solar spectrum can provide the required excitation [1] for particles exposed to sunlight. During sliding contact, the thermal spikes (flash temperatures) at asperities have been reported to be greater than 3000K [9,10], which is high enough for significant excitation.

B. De-excitation Processes

Symmetry breaking can arise from the independent de-excitation processes that occur throughout the bulk and on the surface. The de-excitation rates in the bulk and on the surface, r_B and r_S, are given by,

$$r_B = -hn \tag{1}$$

$$r_S = -kn \tag{2}$$

where n is the concentration ($1/m^3$) of excited electrons, h (1/sec) is the reciprocal of the excited charge carrier lifetime in the bulk, and k is the surface recombination velocity (m/sec).

C. Geometric Scale

Symmetry breaking can occur when the overall bulk and surface de-excitation rates are not of greatly different orders of magnitude. From equations (1) and (2) this occurs at a geometric scale of order k/h. Reported values of h and k for silica-based solids vary over orders of magnitude. However, using mid-range estimates, one finds a geometric roughness scale in the ten-micron range. For example,

$$k/h \approx (10^3 \text{ m/sec})/(10^8 \text{/sec}) \approx 10^{-5} \text{ m} \tag{3}$$

III. MODELING

A. Modeling Assumptions

We do not consider thermal effects on the distributions other than the primary thermal role at the excitation site, and only show steady state results. The latter assumption is reasonable because, in the parameter range of interest, the estimated characteristic time for decay of a thermal pulse is several orders of magnitude longer than the decay time for the pulse of the associated excited electrons. The effect of the internal field generated by

the charge distribution was neglected in most of our computations. Computed estimates show that the decrease in concentration of excited charge carriers arising from the internal field is modest, in our examples about 20%, much less than the uncertainty in the values of the material properties *h* and *k*.

B. Modeling Methods

The surface concentration of excited electrons is calculated by numerical solution of the steady state diffusion equation with appropriate boundary conditions.

$$\frac{\partial n}{\partial t} = D\nabla^2 n + grad\left[\mu En\right] - hn = 0 \tag{4}$$

Neglecting the effect of internal field leads to,

$$D\nabla^2 n - hn = 0 \tag{5}$$

The boundary condition along the bounding surfaces where de-excitation takes place is,

$$Dgrad[n] = -kn \tag{6}$$

The results of the calculation give $n = n(x,y,z)$. Selected results are plotted in Figures 1 and 2.

We performed numerical computations over a wide range of non-dimensional values of the two major parameters affecting the behavior, hR^2/D and kR/D, for two surrogate geometries: a circular right cylinder and a hemispherical region. In each geometry, electrons are excited in one small region (a hot spot). In the cylindrical geometry the hot spot is one face of the cylinder; in the hemispherical region the hot spot is a disk of radius R_0 at the center of the flat face of the hemisphere. De-excitation occurs throughout the bulk of the material, and at a portion of the surface. The de-excitation surface in the cylindrical geometry is the cylindrical surface. In the hemispherical geometry it is the annulus beyond the hot spot on the flat surface.

Most of the computations were done using a second order central difference approximation to the differential equation and a first order approximation for the boundary conditions, solving the equations by iteration. The first order boundary condition was needed for the iteration procedure to converge. From the numerical results sample examinations of the boundary condition to second order were determined, which showed accuracy to within 1%. Some computations were repeated using *Mathematica*, both as a check on the finite difference computations and for three-dimensional displays of some of the information.

C. Numerical Results

Figure 1 shows the distribution of concentration in the cylindrical geometry, for $hR^2/D = 1$ and for a large range of kR/D. For perspective, $hR^2/D = 1$ and $kR/D = 1$ can correspond

to $h = 10^8$ /sec , $k = 10^2$ m/sec, $D = 10^{-4}$ m^2/sec, with $R = 10^{-6}$ m. The cited *h, k,* and *D* values are within reasonable ranges for untreated silica-based solids.

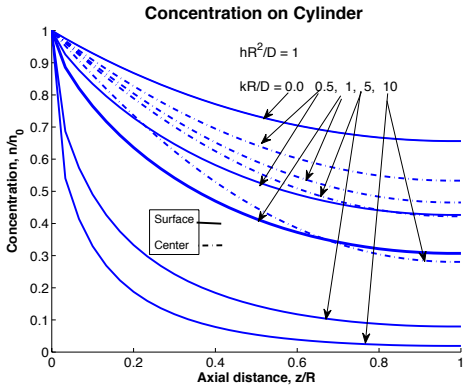

Fig. 1. Plots of the dimensionless concentration of excited electrons in a cylindrical geometry as a function of dimensionless axial distance for a range of parameter values.

In a cylindrical asperity the aspect ratio, *L*/*R*, is a surrogate for the surface roughness. Other results of the modeling, not shown, show that at constant *h* and *k*, the average concentration of excited electrons in the cylindrical asperity decreases with increasing *L*/*R*.

Figure 2 shows the distribution of concentration for the hemispherical geometry, for the same wide range of parameters as shown for the cylindrical geometry in Figure 1. For both the cylindrical and spherical geometries the concentration decreases with increasing values of the surface de-activation, as one expects. Similarly, with constant surface de-activation, the concentration decreases with increasing bulk de-activation; these results are not displayed here.

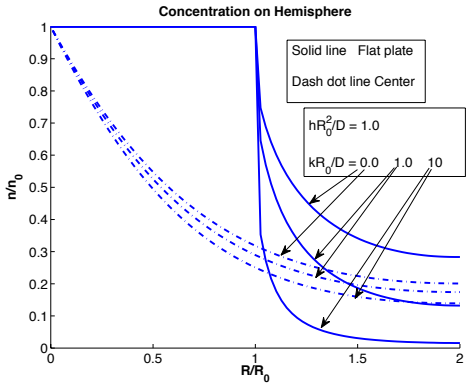

Fig. 2. Plots of the dimensionless concentration of excited electrons along the flat surface and along the centerline of the hemispherical object for a range of parameter values.

For the purpose of visualizing the behavior in the hemispherical geometry, Figure 3 shows the concentration of excited electrons on the flat surface of the hemisphere. The concentration of excited electrons falls rapidly from its value at the hot spot.

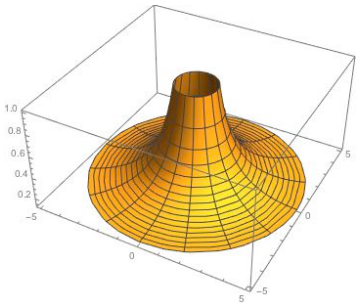

Fig. 3. Dimensionless concentration of excited electrons on the flat surface of the hemispherical object. $R/R_0 = 0.1$; $hR^2/D = 0.1$, $kR/D = 0.01$.

D. Effect on Fermi Energy and Direction of Charge Transfer

The direction of charge transfer between two solids is ultimately determined by the relative positions of the Fermi energies. However, solids subjected to an external photon flux or high local flash temperatures are not in equilibrium and consequently do not have a well-defined Fermi energy. In this case the quasi-Fermi level approximation can be used [11, 12]. This approximation relies on the observation that the time required to equilibrate the excited electrons to the lattice temperature is much less than the time for de-excitation to the valence band and other lower states. This approximation allows one to write the quasi-Fermi energy, E_F, for electrons in an uncharged solid as,

$$E_F = \varepsilon_c^0 + kT \ln\left(\frac{n}{n_c}\right) \tag{7}$$

where ε_c^0 is the electron energy at the conduction band edge, n is the concentration of excited electrons in the conduction band, and $n_c = 2\left[m_e^* k_B T / 2\pi\hbar^2\right]^{3/2}$.

In the present situation, $n << n_C$ so from equation (7) the quasi-Fermi level is within the band gap. Also from equation (7) the quasi-Fermi energy increases with increasing n. Electrons will transfer from objects with greater Fermi energy to objects with lesser Fermi energy. Therefore, the results of the modeling presented here indicate that the direction of electron transfer is from smoother samples to rougher samples. The rate of transfer and total amount of charge transferred depend on the details of the contact and transfer process, which are not considered here.

IV. PRELIMINARY EXPERIMENTAL RESULTS

Preliminary measurements were made of the direction of charge transfer between glass with different surface roughness. Plain glass, uncoated microscope slides obtained from Corning were roughened using 600 grit (16μm diameter) and 120 grit (115μm diameter) silicon carbide paper. Scanning electron microscopy indicated that the "true" surface area of the slide roughened with 120 grit paper was approximately 15% greater than the slide roughened with 600 grit paper.

The slides were subsequently rubbed together and the net charge on each determined using a Faraday cup. In all experiments the smoother slide became positive with respect to the rougher slide. All combinations were tried, and the slide of intermediate roughness became negative with respect to the unroughened slide and positive with respect to the slide roughened with 120 grit paper. The results are summarized in Table 1 as a triboelectric series. These results are in agreement with older studies that have reported some evidence that smoother objects become positively charged with respect to rougher objects. See, for example, Adams [13] and Shaw [14], who reports on experiments of Héséhous [15].

TABLE 1: SUMMARY OF PRELIMINARY TRIBO-ELECTRIC EXPERIMENTS ON GLASS SLIDES OF DIFFERING ROUGHNESS

Sample	*Treatment*	*Triboelectric Series*
Smoothest	As received	+ve
Intermediate roughness	600 grit (16μm)	
Roughest	120 grit (115μm)	-ve

V. CONCLUSIONS

We show that the concentrations of excited electrons in otherwise identical objects of different shapes and sizes can differ because of the different relative magnitudes of surface and volume de-excitation. These differences lead to differences in the Fermi energies and hence to the possibility of charge transfer between objects of identical chemical composition. Charge carriers are predicted to transfer from smoother to rougher and from larger to smaller objects. These predictions are in general agreement with past and present experimental observations.

VI. ACKNOWLEDGEMENTS

The authors gratefully acknowledge the support of Case Western Reserve University. Conversations with colleagues Daniel Lacks, Mohan Sankaran and Kathleen Kash were very helpful. Anu Suppiah and Andrew Wang helped perform the experiments.

REFERENCES

[1] J.C. Angus, I. Greber, K. Kash, "Size-dependent electron chemical potential: Effect on particle charging," *Journal of Electrostatics*, vol. 71, pp.1055-1060, 2013.

[2] P.S.H. Henry, "The role of asymmetric rubbing in the generation of static electricity," *Br. J. Appl. Phys. Suppl*. 2, pp. S31-S36, 1953.

[3] J. Lowell, A.C. Rose-Innes, "Contact electrification," *Adv. Phys*. 29, 947-1023, 1980

[4] C. Liu, A.J. Bard, "Electrostatic electrochemistry at insulators," *Nat. Mater*. vol. 7, pp. 505-509, 2008.

[5] J.A. Wiles, et al., "Effects of Surface Modification and Moisture on the Rates of Charge Transfer between Metals and Organic Materials," *J. Phys. Chem. B* vol. 108, 20296-20302, 2004.

[6] S. Piperno et al., "The Absence of Redox Reactions for Palladium(II) and Copper(II) on Electrostatically Charged Teflon: Relevance to the Concept of 'Cryptoelectrons'," *Angew. Chem. Int. Ed*. vol. 50, pp. 5654 –5657, 2011.

[7] H.T. Baytekin, et al., "The Mosaic of Surface Charge in Contact Electrification," *Science* 333, pp. 308-312, 2011.

[8] D.J. Lacks, M. Sankaran, "Contact electrification of insulating materials," *J. Phys. D: Appl. Phys*. vol.44, pp. 453001-453015, 2011.

[9] M. Akbulut et al., "Triboelectrification between Smooth Metal Surfaces Coated with Self-Assembled Monolayers (SAMs)," *J. Phys. Chem. B.* vol. 110, pp.22271-22278, 2006.

[10] M. Kalin, "Influence of flash temperatures on the tribological behaviour in low-speed sliding: a review," *Mat. Sci. & Eng. A*, vol. 374, pp. 390-397, 2004.

[11] M. Fox, *Optical Properties of Solids*, Oxford University Press, Oxford, 2010, p. 119.

[12] S.M. Sze, K.K. Ng, *Physics of Semiconductor Devices*, Wiley Interscience, Hoboken, NJ, 2007, pp. 90-91.

[13] George Adams, "Essay on Electricity," London, 1785, p. 15.

[14] P.E. Shaw, "Experiments on Tribo-Electricity: I. The Tribo-Electric Series," *Proc. Roy. Soc. London. Series A. Containing Papers of a Mathematical and Physical Character,* vol. 94, pp. 16-33, 1917.

[15] N.A. Héséhous, *Jurn. Russk. Fisik-Chimicesk. Obscestva* vol. 34, pp. 1-15, 1902; *Jurn. Russk. Fisik-Chimicesk. Obscestva* vol. 35, pp. 575-80, 1903; *Jurn. Russk. Fisik-Chimicesk. Obscestva* vol. 37, pp. 29-33, 1905.